


Article

A Real-Time Simulink Interfaced Fast-Charging Methodology of Lithium-Ion Batteries under Temperature Feedback with Fuzzy Logic Control

Muhammad Umair Ali ¹, Sarvar Hussain Nengroo ¹ , Muhamad Adil Khan ¹, Kamran Zeb ^{1,2}, Muhammad Ahmad Kamran ³ and Hee-Je Kim ^{1,*}

¹ School of Electrical Engineering, Pusan National University, Busandaehak-ro 63 Beon-gil 2, Busan 46241, Korea; umairali.m99@gmail.com (M.U.A.); ssarvarhussain@gmail.com (S.H.N.); engradilee@gmail.com (M.A.K.); kami_zeb@yahoo.com (K.Z.)

² School of Electrical Engineering and Computer Science, National University of Sciences and Technology, Islamabad 44000, Pakistan

³ Department of Cogno-Mechatronics Engineering, Pusan National University, Busandaehak-ro 63 Beon-gil 2, Busan 46241, Korea; malik.pieas@gmail.com

* Correspondence: heeje@pusan.ac.kr; Tel.: +82-51-510-2364

Received: 2 April 2018; Accepted: 1 May 2018; Published: 2 May 2018



Abstract: The lithium-ion battery has high energy and power density, long life cycle, low toxicity, low discharge rate, more reliability, and better efficiency compared to other batteries. On the other hand, the issue of a reduction in charging time of the lithium-ion battery is still a bottleneck for the commercialization of electric vehicles (EVs). Therefore, an approach to charge lithium-ion batteries at a faster rate is needed. This paper proposes an efficient, real-time, fast-charging methodology of lithium-ion batteries. Fuzzy logic was adopted to drive the charging current trajectory. A temperature control unit was also implemented to evade the effects of fast charging on the aging mechanism. The proposed method of charging also protects the battery from overvoltage and overheating. Extensive testing and comprehensive analysis were conducted to examine the proposed charging technique. The results show that the proposed charging strategy favors a full battery recharging in 9.76% less time than the conventional constant-current–constant-voltage (CC/CV) method. The strategy charges the battery at a 99.26% state of charge (SOC) without significant degradation. The entire scheme was implemented in real time, using Arduino interfaced with MATLABTM Simulink. This decrease in charging time assists in the fast charging of cell phones and notebooks and in the large-scale deployment of EVs.

Keywords: fast charging; multistage current charging; lithium-ion battery; fuzzy logic controller; life cycle

1. Introduction

The extensive use of petrol, diesel, and other fossil fuels in automobiles has had adverse effects on global warming and greenhouse gas (GHG) emissions [1–3]. In addition to global warming and GHG, the fossil fuel prices are increasing rapidly, which is a setback in the automobile industry. To overcome these economic and pollution problems, electric vehicles (EVs) and plug-in hybrid electric vehicles (PHEVs) are becoming a transportation secondary option [4–8]. By 2050, the annual sale of EVs and PHEVs is expected to reach approximately 100 million [9]. This growth in the demand for EVs and PHEVs has captivated many researchers to design rechargeable batteries [10–12]. Lithium-ion, lead acid, and nickel–metal hydride (NiMH) batteries have been adopted as energy charge storage devices in

EVs and PHEVs [13]. The lithium-ion battery is preferred because of its long life cycle, reliability, high energy density, low toxicity, low self-discharge rate, high power density, and high efficiency [14–17].

A single cell of a lithium-ion battery has a low voltage. Therefore, a combination of cells is used in series to boost the voltage, but its outcomes are deep discharging, overcharging, and a decrease in battery storage capacity. The undercharged and overcharged conditions influence the life cycle of a battery [18]. The undercharged condition prevents reaching the maximum storage capacity, and the overcharged condition damages the battery physically. In addition to these deficiencies, a critical concern is the long charging time.

In recent years, decreasing the charging time of lithium-ion batteries without affecting their capacity and physical condition has been a serious concern for researchers. For the charging of lithium-ion batteries, different charging techniques, such as constant current and constant voltage (CC/CV), pulse charging (PC) algorithm, model-based charging, and multistage current charging algorithm (MSCC), have been reported [19–34]. The CC/CV techniques is computationally efficient and can be implemented easily. This technique has two main steps. In the first step, a constant current is provided to the battery until the battery voltage reaches the preset voltage. In the second interval, the constant voltage mode is turned ON, and the battery current begins to decrease exponentially until it reaches a preset small charging current [19]. In this method, different sensors are required to check the current and battery voltage. Many variants of the CC/CV charging algorithm have been reported, e.g., the double-loop charger (DL-CC/CV). In the DL-CC/CV technique, the role of the current sensor is eliminated by taking the feedback of the battery voltage [20]. Tsang and Chan presented the concept of the PC algorithm. In the PC algorithm, the main part is to control the frequency of the pulse to check the response of the current [21]. The optimal frequency can be achieved at low battery impedance, resulting in the maximum charging current.

Similarly, the MSCC algorithm has been implemented to charge the battery, in which different charging currents are applied at different intervals, but the hindrance is how to determine the appropriate current for different charging intervals. For this purpose, a controller or computer is necessary to calculate the values. The Taguchi methodology decides the charging current by estimating the state of charge (SOC) of the battery [22]. In the model-based charge control, the estimation of the SOC is a crucial step. Several previous studies have discussed equivalent circuit models to estimate the SOC. However, the SOC and capacity determination is still a challenging task because it is difficult to measure it with sensors. Recently, Wei and coauthors [23–25] presented recursive online models to estimate the SOC of a lithium-ion battery. Wei et al. [23] indicated the problem of biased results for the estimation of the SOC using conventional identification methods in the model-based charging technique. They proposed a recursive least square-based Frisch scheme to enhance the model identification and estimation of the SOC in the presence of noise. In their subsequent work, Wei et al. [24] proposed a multi-timescale method for dual estimation of the SOC with the online battery model. Their results suggest that this method determines SOC and capacity with fast convergence and high accuracy. In a recent study of Wei et al. [25], a novel recursive total least square-based observer method was proposed to suppress the noise effect in a model. The authors were able to estimate the SOC with high accuracy. However, the equivalent circuit model for a lithium-ion battery varies from a simple representation to a very complex mathematical form. A simple model can simulate the dynamic characteristics of the battery up to a certain accuracy. On the other hand, a complex model shows much better results as compared to the simple one, but these are difficult to implement in real time.

Furthermore, Guo et al. [26] reported another way to improve the charging time and life cycle using a universal voltage protocol. Zhang et al. [27] proposed that a dynamic optimization algorithm can be utilized to determine the optimal charging time. Liu et al. [28] implemented the ant colony algorithm to find the optimal current to charge a lithium-ion battery. In addition to these methodologies, a fuzzy logic controller (FLC) could be beneficial [29–34]. Huang et al. [29] used FLC to find the charging current for different intervals, in which the inputs of the controller were the temperature rise and the deviation of the temperature rise. The proposed methodology increased the charging

efficiency of the battery but required more time to charge it. Lee et al. [30,34] also implemented the FLC to equalize the voltages of a cell in a string. This reduced the equalization time of voltages in a string compared to the conventional process. Ho et al. [31] implemented the FLC with the Taguchi method to improve the charging time. The Taguchi method was utilized to determine the optimal output membership function of the FLC. The temperature of the battery and the gradient of temperature rise were the inputs of the FLC. Lyn et al. [32] used battery voltage and charging current as inputs of the FLC, and the longer time consumption for higher charging efficiency was the limitation of this methodology. Hsieh et al. [33] used the FLC by monitoring the charging state of the battery and replaced the CV mode of the CC/CV method with the proposed methodology. This only reduces the charging time of the CV mode; however, the overall charging time improvement was not so high.

This paper proposes the MSCC technique embedded with fuzzy logic and temperature feedback for series-connected lithium-ion batteries. The voltage and temperature were fed to the controller to find the optimal charging current within the safe temperature limit. The proposed method charges the battery in a faster way. Also, the temperature control unit avoids the effects of fast charging on the aging mechanism and protects the battery from an overvoltage condition. The proposed technique was implemented on a three-cell lithium-ion battery. Figure 1 presents the general diagram of the proposed system. The FLC and temperature control units were implemented using Arduino MEGA 2560 interfaced with MATLAB™ Simulink 2017. Extensive testing and comprehensive analysis were done to validate the proposed technique. The charging time, charging capacity, and life cycle of the battery are discussed.

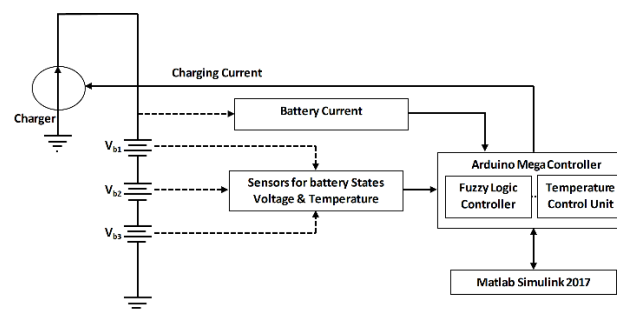


Figure 1. General diagram of the proposed battery-charging system.

The paper is organized as follows. Section 2 describes the fuzzy logic control temperature-feedback battery-charging system. Section 3 presents the experimental setup. Section 4 discusses the results. The conclusions are summarized in the last section.

2. Theory

2.1. Background of Fuzzy Logic for the Lithium-Ion Battery

The lithium-ion battery is a very complex nonlinear system. Therefore, it is very difficult to determine the precise mathematical model of the lithium-ion battery. Consequently, it is necessary to use a controller, which does not require a precise mathematical model of a battery. In this regard, a fuzzy logic controller is a better choice because it is used for nonlinear mapping of the input data to scalar output data. In this study, a fuzzy logic controller was implemented to enhance the charging efficiency of a lithium-ion battery.

A fuzzy logic-controlled system can be divided into four parts: fuzzification, fuzzy rule base, fuzzy inference engine, and defuzzification [35–38]. Figure 2 presents a generic overview of the FLC.

Fuzzification: This converts the input true data value into fuzzy linguistic sets, using a membership function. **Fuzzy rule base:** This is the main component of the system and the operating control of the system designed in it. In addition, the control law parameters of the system are stored in

a database. This requires considerable professional skill and experience to design a fuzzy rule base. Inference engine: This is an operating method that converts a fuzzy linguistic input to a fuzzy linguistic output according to the control law defined in a fuzzy rule base. Defuzzification: This converts the fuzzy linguistic output to the true value according to the membership function.

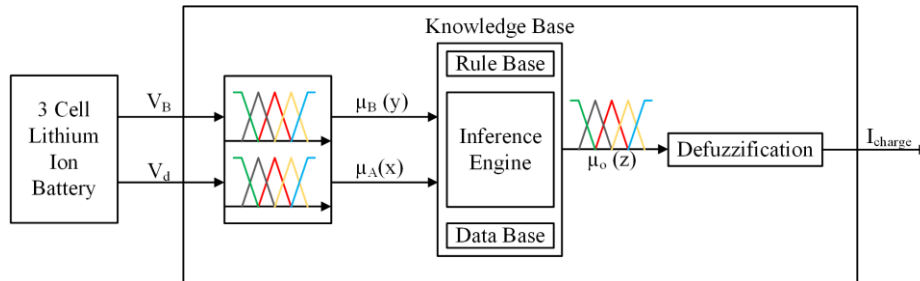


Figure 2. Fuzzy logic system; V_B = lowest single-cell voltage of the string, V_d = highest voltage difference between two cells of a battery, μ_B = fuzzy variable of V_B , μ_A = fuzzy variable of V_d , I_{charge} = Output Charging Current, and μ_o = fuzzy variable of I_{charge} .

2.2. Fuzzy Logic Controller Design

A fuzzy logic base Arduino controller is proposed to control the charging current of the battery. The fuzzy controller has two inputs. The first is the lowest single-cell voltage of the string (V_B), and the other one is the highest voltage difference between the two cells of the battery (V_d), as shown in Figure 2. The fuzzifier changes the input data to linguistic fuzzy sets, and the inference engine then determines the optimal value using the input fuzzy data and rule base. The rule base, which is stored in the database of the system, is listed in Table 1. Finally, the defuzzifier changes the fuzzy linguistic sets of the output in the numerical value of the charging current I_{charge} .

Table 1. Rule base for linguistic variables. VS, S, M, L, and VL are very small, small, medium, large and very large respectively.

		Voltage Difference, V_d					
		Output	VS	S	M	L	VL
Cell Voltage, V_B	VS	VS	M	L	VL	VL	
	S	VS	M	L	VL	VL	
	M	VS	M	L	VL	VL	
	L	VS	S	M	L	VL	
	VL	VS	S	M	L	VL	

The five linguistic variables used in Table 1 are: VS (very small), S (small), M (medium), L (large), and VL (very large). When the variable appears on the horizontal top row in Table 1 (blue color), it shows the voltage difference; similarly, when appearing in the leftmost column of Table 1 (green color), it shows the battery voltage levels, and, when appearing inside Table 1 (black color), it represents different stages of the charge current. Lee et al. [30] used a similar set of rule bases. The fuzzy variables for V_B , V_d , and I_{charge} are μ_B , μ_A , and μ_o , respectively. Figure 3 shows the sets of membership functions of the fuzzy variables.

current does not affect the battery life. For that particular reason, the temperature control unit was added which continuously measures and adjusts the current value accordingly. The detail of the temperature control unit are discussed in Section 2.3.

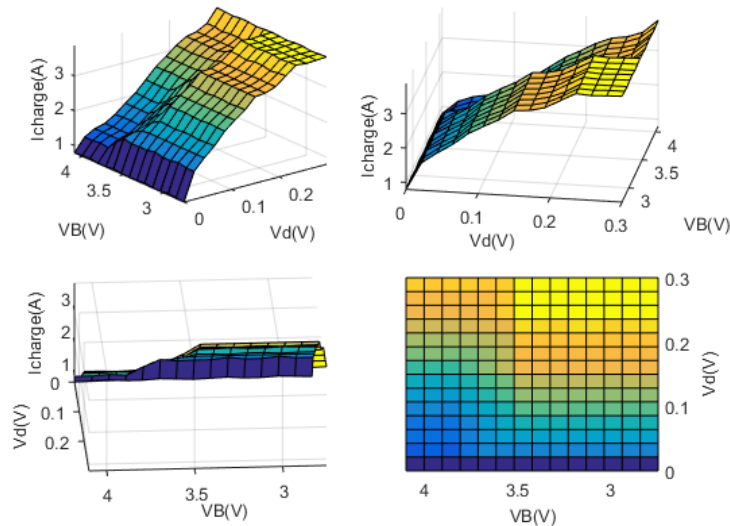


Figure 4. Output surface (I_{charge}) of the fuzzy logic controller according to V_d and V_B .

2.3. Temperature Control Unit

The basic function of the temperature control unit is to maintain the battery temperature to a safe limit predefined by the manufacturer. Figure 5 shows the temperature control flow chart of the Samsung ICR18650-26F lithium-ion battery. In the Samsung ICR18650-26F lithium-ion battery, the charging temperature limit is 0–45 °C [39]. Hence, the temperature upper limit check was set to 40 °C to be safe.

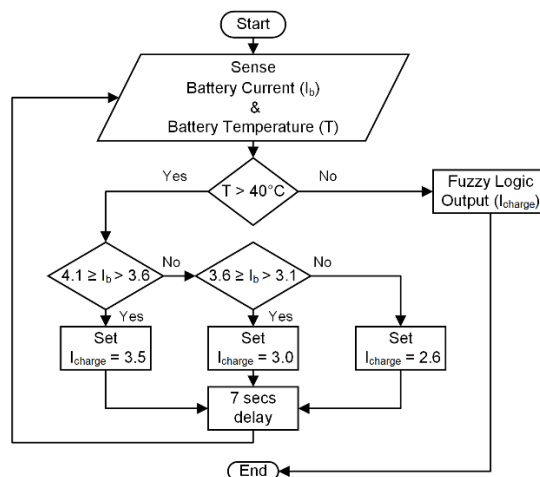


Figure 5. Temperature control flow chart.

The temperature control unit continuously senses the battery current (I_b) and the battery temperature (T). If the temperature is below 40 °C, the fuzzy logic output current is supplied to the battery. When the battery temperature (T) crosses the 40 °C limit, the controller compares the battery current (I_b) with the range defined in the flow chart. If I_b lies between 3.6 and 4.1 A, the controller sets I_{charge} to 3.5 A and continuously checks the temperature every 7 s to verify whether the temperature is increasing or is maintained at the same level. If the temperature is outside the defined limits,

it reduces the I_{charge} to 3 A. Similarly, if the temperature is at the same level, i.e., greater than the defined limit, the controller sets I_{charge} to 2.6 A, which is the safe current for a battery, as defined by the manufacturer [39].

3. Experimental Setup

The Samsung ICR18650-26F lithium-ion battery was used in the current experimental setup to analyze the methodology. A string of three cells connected in series was used. Figure 6 shows the experimental setup, with different sensors used to measure and monitor the parameters, such as battery voltage, charge current, and temperature.

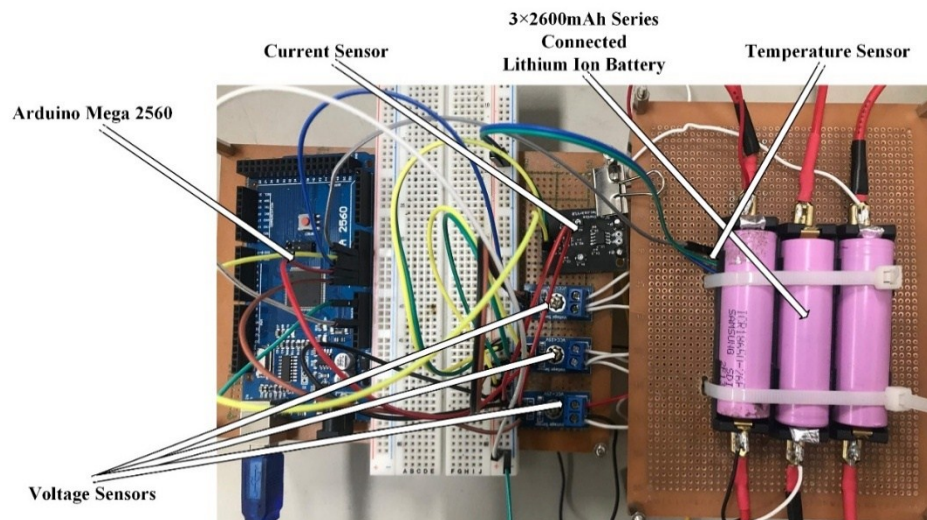


Figure 6. Hardware configuration of the fast-charging system.

The proposed technique was implemented using Arduino Mega 2560. MATLAB™ Simulink 2017 was used to program the controller; the real-time data were measured and monitored in MATLAB™ Simulink. The data were also recorded in the workspace. Figures 7–9 present the Simulink configuration of the battery-charging system.

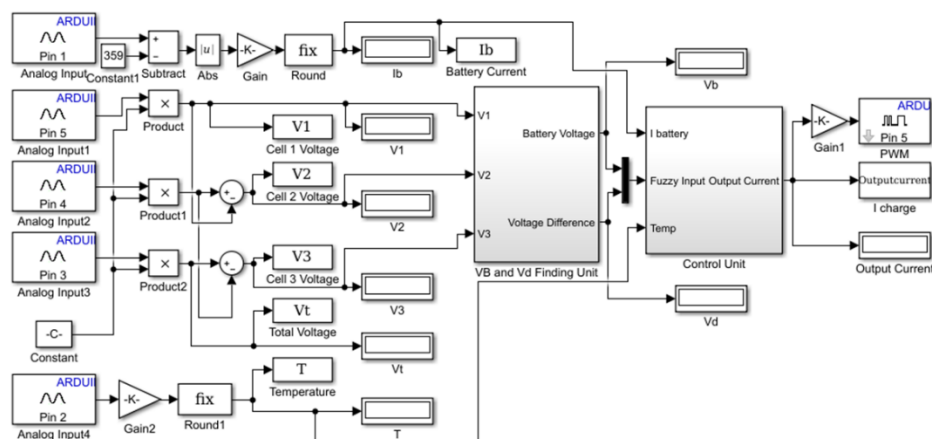


Figure 7. Real-time Simulink configuration.

Figure 7 shows the real-time measuring and monitoring system of the battery charging on Simulink MATLAB™. The sensor output to the Arduino analogue pins were converted to true values.

These values were then passed to module 2, as shown in Figure 8. Figure 8 shows the scheme followed to find V_d and V_B .

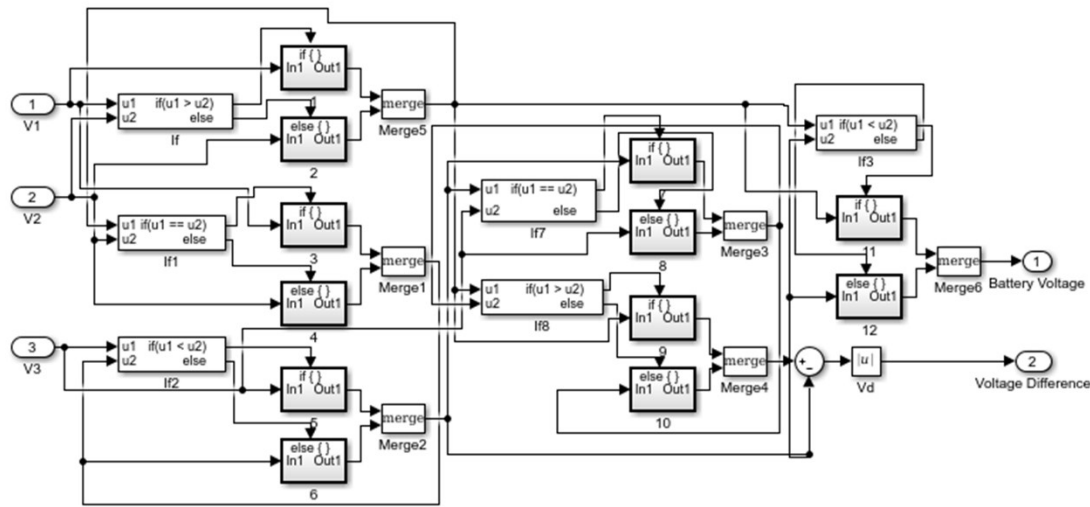


Figure 8. Finding the largest voltage difference of the cells (V_d) and the lowest battery voltage (V_B).

Figure 9 presents the fuzzy logic controller and temperature control unit. V_d and V_B are the inputs of the fuzzy logic controller. The output of the fuzzy logic controller is the input of the temperature control unit along with the battery temperature (T) and the battery current (I_b). The temperature control unit was programmed using the state flow chart of MATLABTM.

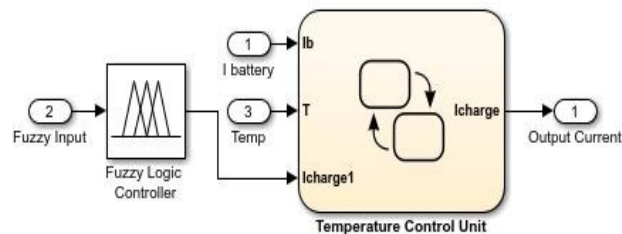


Figure 9. Fuzzy logic controller and temperature control unit.

4. Results and Discussion

A wide range of electrical equipment, such as notebooks, cell phones, MP3 players, and EVs, are operated by batteries. These batteries take several hours to charge, which leads to a long out-of-service time. Therefore, a reduction in battery charging time has become a significant issue. The basic aim of fast charging is to charge the battery in a fast, safe, and efficient manner.

Figure 1 gives a general overview of the proposed fast-charging methodology. Three series of connected lithium-ion cells were used. The sensors feed the states of the battery to the controller, and the controller is interfaced with MATLABTM Simulink. Figure 2 shows the fuzzy logic control system in detail. Table 1 and Figure 3 present the rule base and membership functions values, respectively. Figure 4 shows the relationship between the inputs and output of the FLC. Figure 5 presents a flow chart of the temperature control unit of the battery, and Figure 6 shows the experimental setup of the proposed charging system. Figures 7–9 present the MATLABTM Simulink measuring, monitoring, and control system. Figures 10 and 11 present the charging profile of the battery using the conventional and proposed way of charging, respectively. Figure 12 shows the current profile of battery charging using the proposed technique. Figures 13 and 14 show the temperature during the proposed charging methodology. Figures 15–17 present the battery capacity and discharging

curves. The comparison of the life cycle tests between the proposed and the conventional charging methodology is shown in Figure 18. Table 2 summarizes the results of this research.

Several experiments were performed with different initial cell voltages to verify the proposed technique. First, the battery was charged using the CC–CV method (defined by the manufacturer) to determine its normal charging time [39]. The initial cell voltages were $V_1 = 3.391$ V, $V_2 = 3.263$ V, and $V_3 = 3.353$ V. Figure 10 shows the conventional charging profile of the battery. The process took 8997 s (2.5 h) to fully charge the battery (see Figure 10); the same charging time (2.5 h) was also mentioned by the manufacturer [39].

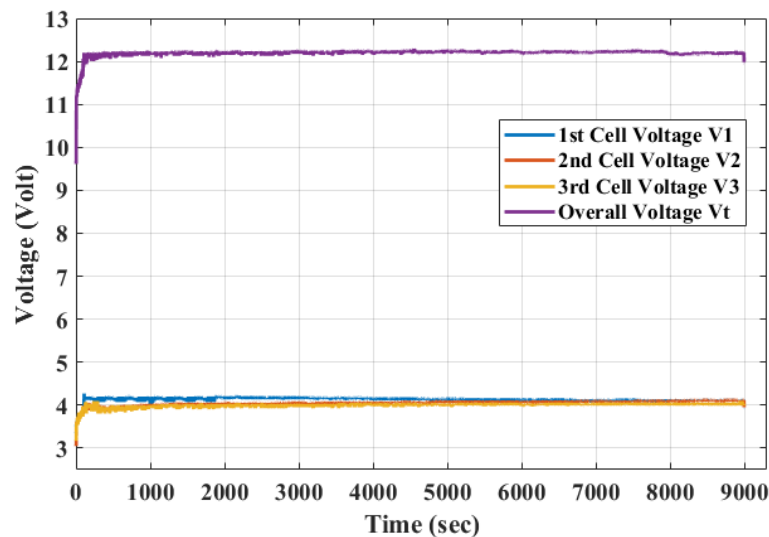


Figure 10. Charging profile of a lithium-ion battery at 1 C.

The proposed charging technique was applied to a three-cell battery with different initial cell voltages. In this case, the initial voltages were $V_1 = 3.393$ V, $V_2 = 3.367$ V, and $V_3 = 3.273$ V. Figures 11 and 12 show the charging profiles using the proposed technique.

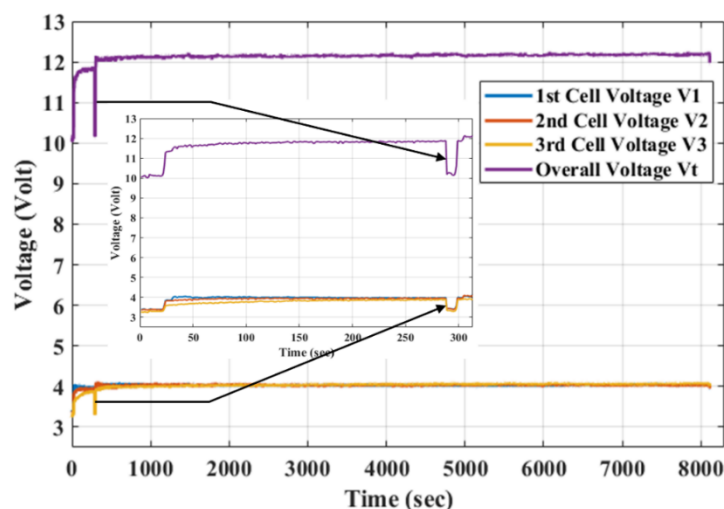


Figure 11. Charging voltage profile of the lithium-ion battery using the proposed technique.

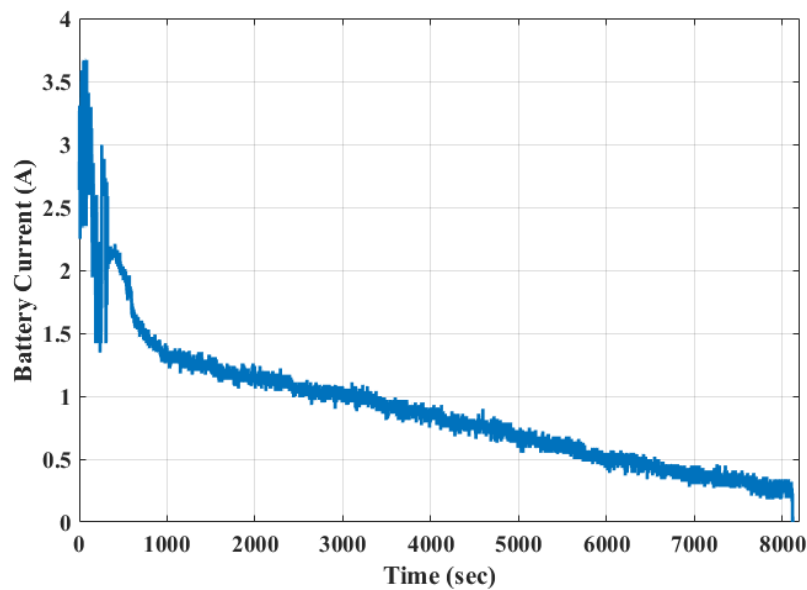


Figure 12. Current profile of the lithium-ion battery using the proposed technique.

The battery took 8118 s (2.25 h) to charge, as shown in Figures 11 and 12. This was almost 15 min (879 s) less than the normal charging time. The spike shown in the graph was attributed to the over-temperature limit. When the temperature increased to more than 40 °C, the charging current reduced to manage the temperature, as described in Section 2.3 and shown in the magnified part of Figure 11. The temperature was monitored and measured using a thermocouple and FLUKE VT04A visual infrared IR thermometer. The thermocouple provided the input directly to the controller, and an IR thermometer was used to monitor the temperature manually. Figure 13 presents some of the images captured during the proposed charging using the IR thermometer.

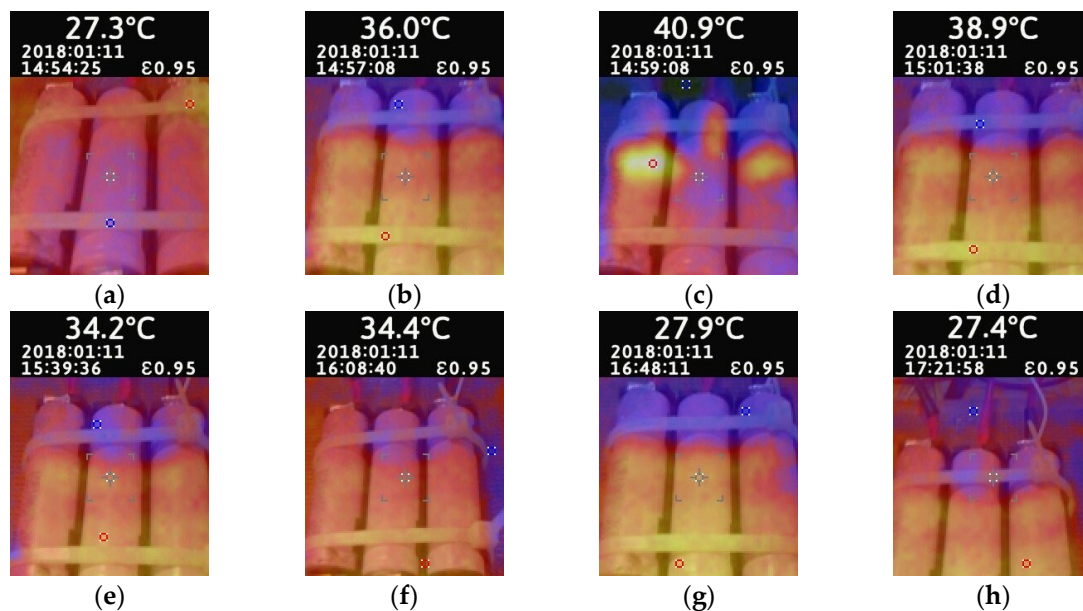


Figure 13. Temperature measurements during the proposed charging scheme at different time intervals, (a) at $t = 0$ s, (b) at $t = 163$ s, (c) at $t = 283$ s, (d) at $t = 433$ s, (e) at $t = 2711$ s, (f) at $t = 4455$, (g) at $t = 6862$, and (h) after complete charging.

The temperature of the cells was 27.3 °C at the beginning of charging, as shown in Figure 13a. As charging began, the temperature started to rise because of the high charging current and reached 40.9 °C (Figure 13c). The temperature control unit then reduced the charging current to control the temperature of the battery. Owing to the reduction in the charging current, a spike in the charging curve was observed (Figure 11). The temperature then began to decrease because the battery started to draw a low current (Figure 13e–g). After charging, the temperature of the battery was 27.4 °C, as shown in Figure 13h. The temperature-versus-time graph of the battery during charging is shown in Figure 14.

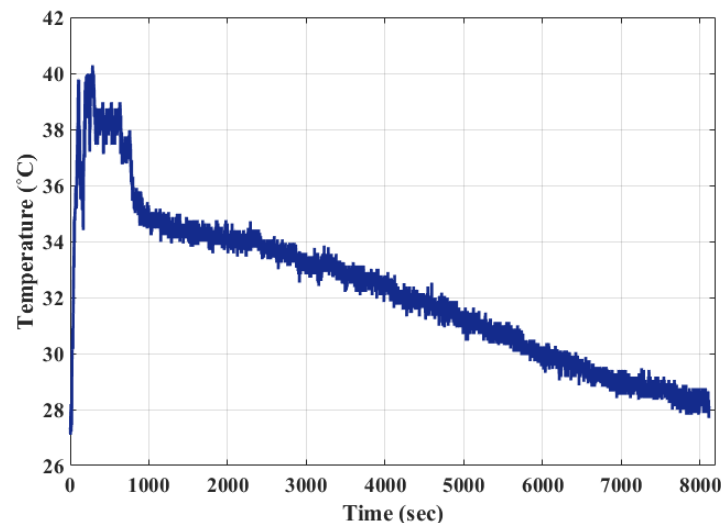


Figure 14. Temperature of the battery during the proposed charging.

The charging capacity of the battery using this technique was approximately 99.26%, which was the same as that of a 1 C charge. The proposed technique did not reduce the life cycle of the battery because the temperature of the battery remained within the safe limit (below 45 °C). Figure 15 shows the discharging curve of the battery at 0.23 C (0.6 A).

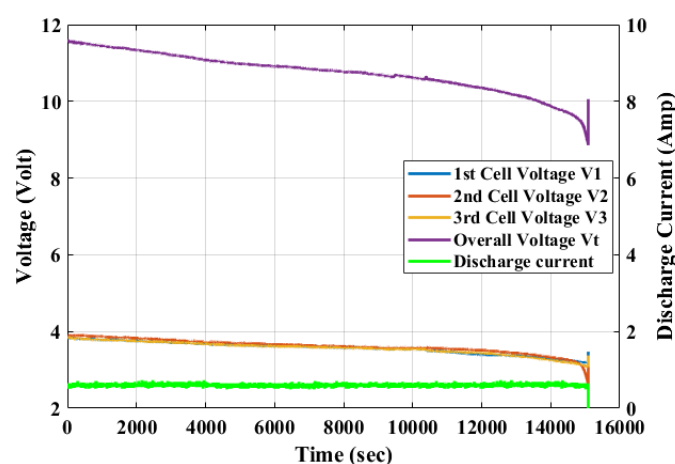


Figure 15. Discharging curve at 0.23 C.

Figure 16 shows the relationship between the voltage and the capacity (mAh) of the battery during the discharging condition.

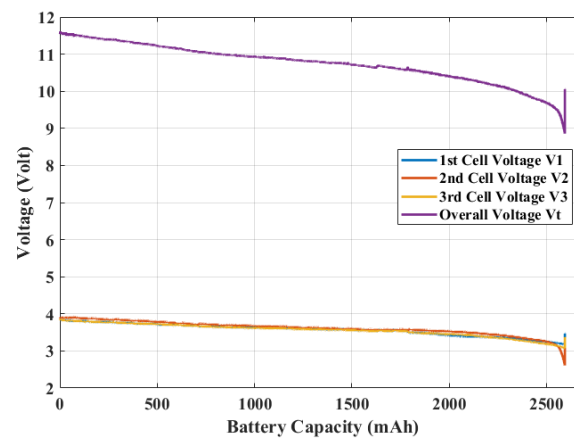


Figure 16. Battery capacity curve.

Figure 17 presents the discharging curves of the battery at 0.38 C of 26th cycle, 0.8 C of 24th cycle, 1 C of 21st cycle, and 2 C of 29th cycle. These curves show that the battery was charged almost at its full capacity (2600 mAh) using the proposed technique.

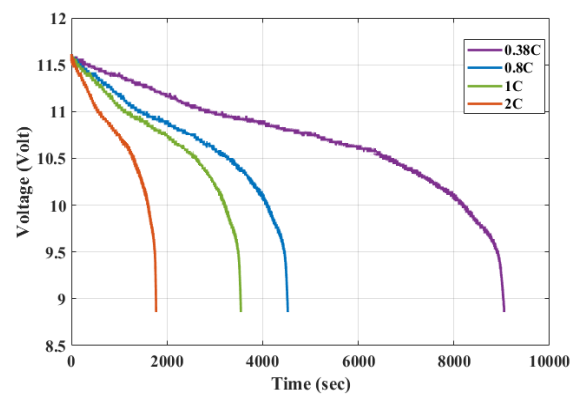


Figure 17. Discharging curves at 0.38 C of 26th cycle, 0.8 C of 24th cycle, 1 C of 21st cycle, and 2 C of 29th cycle.

Using the proposed technique, the charging time of the battery was decreased without affecting its life cycle and charge capacity. A total of 50 experiments were performed to validate the proposed technique. The comparison of cycle life tests between the proposed and the CCCV technique is shown in Figure 18.

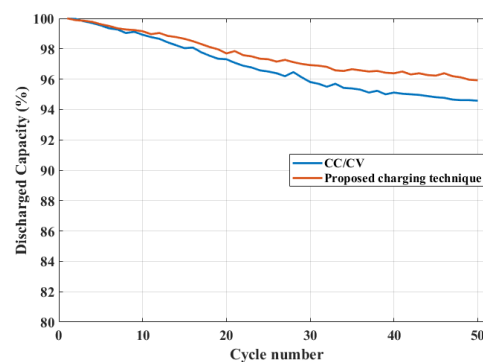


Figure 18. Comparison of cycle life tests between the proposed and the CCCV technique.

Some other experiments were performed by changing the number of fuzzy variables and the value of the membership functions. By adopting three fuzzy variables, the decrease in the charging time was 3 to 4 min, and by increasing the value of the membership function, the temperature increased at a rapid pace. In the proposed technique, five fuzzy variables were selected with the membership value mentioned in Table 1 and Figure 3. Different experiments were performed with different initial voltages. The results are shown in Table 2.

Table 2. Comparison of the charging techniques.

Method	Worst Time (s)	Average Time (s)	Best Time (s)	Charging Efficiency (%)
Conventional Charging [39]	9013	8983	8921	98.06
Proposed Technique	8148	8106	8056	98.11
Improvement	9.60%	9.76%	9.69%	0.05

In recent years, many intelligent charging methods have been applied using microprocessors and computers. One of these techniques is to control the charging process by sensing the tuning points. These tuning points have been selected based on the battery temperature, voltage, and lapsed charging time [40]. The control algorithm changes the charging behavior only at the tuning points, and the period outside the tuning points is unaffected. The ant colony algorithm was used to optimize the MSCC profile [28]. This optimization algorithm does not use the real-time measurements of the state of the battery to change the charging current, but rather finds the best charging profile for the entire process. Saberi et al. [41] applied a genetic algorithm (GA) to solve the charging problem for the lithium-ion battery. The performance of the GA was dependent on the system accuracy; the robustness of the GA decreased because of the noise and time variance properties of the battery. Chen et al. [42] used the grey prediction technique for battery charging without taking the temperature into consideration. The advantages of the proposed methodology over the previous techniques are that it is easy to implement and that all battery states are considered during the charging state. Therefore, the battery can be protected from overvoltage, overcharging, and overheating conditions. The results show an almost 15 min decrease in the charging time without affecting the capacity and life cycle, which is significant for the battery life.

5. Conclusions

A real-time multistage current charging technique embedded with fuzzy logic and temperature feedback was implemented in this paper. The proposed technique was designed and programmed in MATLABTM Simulink. The methodology was implemented using a three-cell lithium-ion battery. The results revealed a 9.76% reduction in the charging time compared to the conventional way of charging. This method of charging does not decrease the charging capacity and charging efficiency. The temperature feedback was introduced to protect the battery from overheating. The experimental results show that the proposed charging technique for charging a battery is faster and safer than the conventional techniques.

Author Contributions: Hee-Je Kim and Muhammad Umair Ali have conceptualized the idea of this study. The experimental setup has developed and analyzed by Muhammad Umair Ali and Sarvar Hussain Nengroo. Muhammad Adil Khan and Kamran Zeb contributed in the controller programming. The initial manuscript prepared by Muhammad Umair Ali and Muhammad Ahmad Kamran. Hee-Je Kim supervised and finalized the research manuscript.

Acknowledgments: The work was supported by BK 21 plus.

Conflicts of Interest: The authors declare no conflict of interest.

References

- Hannan, M.; Azidin, F.; Mohamed, A. Hybrid electric vehicles and their challenges: A review. *Renew. Sustain. Energy Rev.* **2014**, *29*, 135–150. [\[CrossRef\]](#)
- Budzianowski, W.M. Negative carbon intensity of renewable energy technologies involving biomass or carbon dioxide as inputs. *Renew. Sustain. Energy Rev.* **2012**, *16*, 6507–6521. [\[CrossRef\]](#)
- Sulaiman, N.; Hannan, M.; Mohamed, A.; Majlan, E.; Daud, W.W. A review on energy management system for fuel cell hybrid electric vehicle: Issues and challenges. *Renew. Sustain. Energy Rev.* **2015**, *52*, 802–814. [\[CrossRef\]](#)
- Poullikkas, A. Sustainable options for electric vehicle technologies. *Renew. Sustain. Energy Rev.* **2015**, *41*, 1277–1287. [\[CrossRef\]](#)
- Hofmann, J.; Guan, D.; Chalvatzis, K.; Huo, H. Assessment of electrical vehicles as a successful driver for reducing CO₂ emissions in china. *Appl. Energy* **2016**, *184*, 995–1003. [\[CrossRef\]](#)
- Casals, L.C.; Martinez-Laserna, E.; García, B.A.; Nieto, N. Sustainability analysis of the electric vehicle use in europe for CO₂ emissions reduction. *J. Clean. Prod.* **2016**, *127*, 425–437. [\[CrossRef\]](#)
- Abdul-Manan, A.F. Uncertainty and differences in ghg emissions between electric and conventional gasoline vehicles with implications for transport policy making. *Energy Policy* **2015**, *87*, 1–7. [\[CrossRef\]](#)
- Sathishkumar, P.; Piao, S.; Khan, M.A.; Kim, D.-H.; Kim, M.-S.; Jeong, D.-K.; Lee, C.; Kim, H.-J. A blended sps-esps control dab-ibdc converter for a standalone solar power system. *Energies* **2017**, *10*, 1431. [\[CrossRef\]](#)
- Tanaka, N. *Technology Roadmap: Electric and Plug-In Hybrid Electric Vehicles*; International Energy Agency, Technical Report; International Energy Agency: Paris, France, 2011.
- Herrmann, F.; Rothfuss, F. Introduction to hybrid electric vehicles, battery electric vehicles, and off-road electric vehicles. In *Advances in Battery Technologies for Electric Vehicles*; Elsevier: Cambridge, UK, 2015; pp. 3–16.
- Shareef, H.; Islam, M.M.; Mohamed, A. A review of the stage-of-the-art charging technologies, placement methodologies, and impacts of electric vehicles. *Renew. Sustain. Energy Rev.* **2016**, *64*, 403–420. [\[CrossRef\]](#)
- Yong, J.Y.; Ramachandaramurthy, V.K.; Tan, K.M.; Mithulanathan, N. A review on the state-of-the-art technologies of electric vehicle, its impacts and prospects. *Renew. Sustain. Energy Rev.* **2015**, *49*, 365–385. [\[CrossRef\]](#)
- Manzetti, S.; Mariasiu, F. Electric vehicle battery technologies: From present state to future systems. *Renew. Sustain. Energy Rev.* **2015**, *51*, 1004–1012. [\[CrossRef\]](#)
- Saw, L.H.; Ye, Y.; Tay, A.A. Integration issues of lithium-ion battery into electric vehicles battery pack. *J. Clean. Prod.* **2016**, *113*, 1032–1045. [\[CrossRef\]](#)
- Rao, Z.; Wang, S.; Zhang, G. Simulation and experiment of thermal energy management with phase change material for ageing lifepo4 power battery. *Energy Convers. Manag.* **2011**, *52*, 3408–3414. [\[CrossRef\]](#)
- Scrosati, B.; Garche, J. Lithium batteries: Status, prospects and future. *J. Power Sources* **2010**, *195*, 2419–2430. [\[CrossRef\]](#)
- Jugović, D.; Uskoković, D. A review of recent developments in the synthesis procedures of lithium iron phosphate powders. *J. Power Sources* **2009**, *190*, 538–544. [\[CrossRef\]](#)
- Horiba, T. Lithium-ion battery systems. *Proc. IEEE* **2014**, *102*, 939–950. [\[CrossRef\]](#)
- Hussein, A.A.-H.; Batarseh, I. A review of charging algorithms for nickel and lithium battery chargers. *IEEE Trans. Veh. Technol.* **2011**, *60*, 830–838. [\[CrossRef\]](#)
- Tsang, K.; Chan, W. Current sensorless quick charger for lithium-ion batteries. *Energy Convers. Manag.* **2011**, *52*, 1593–1595. [\[CrossRef\]](#)
- Chen, L.-R. A design of an optimal battery pulse charge system by frequency-varied technique. *IEEE Trans. Ind. Electron.* **2007**, *54*, 398–405. [\[CrossRef\]](#)
- Vo, T.T.; Chen, X.; Shen, W.; Kapoor, A. New charging strategy for lithium-ion batteries based on the integration of taguchi method and state of charge estimation. *J. Power Sources* **2015**, *273*, 413–422. [\[CrossRef\]](#)
- Wei, Z.; Meng, S.; Xiong, B.; Ji, D.; Tseng, K.J. Enhanced online model identification and state of charge estimation for lithium-ion battery with a fbcrs based observer. *Appl. Energy* **2016**, *181*, 332–341. [\[CrossRef\]](#)
- Wei, Z.; Zhao, J.; Ji, D.; Tseng, K.J. A multi-timescale estimator for battery state of charge and capacity dual estimation based on an online identified model. *Appl. Energy* **2017**, *204*, 1264–1274. [\[CrossRef\]](#)

25. Wei, Z.; Zou, C.; Leng, F.; Soong, B.H.; Tseng, K.-J. Online model identification and state-of-charge estimate for lithium-ion battery with a recursive total least squares-based observer. *IEEE Trans. Ind. Electron.* **2018**, *65*, 1336–1346. [[CrossRef](#)]
26. Guo, Z.; Liaw, B.Y.; Qiu, X.; Gao, L.; Zhang, C. Optimal charging method for lithium ion batteries using a universal voltage protocol accommodating aging. *J. Power Sources* **2015**, *274*, 957–964. [[CrossRef](#)]
27. Zhang, S.; Zhang, C.; Xiong, R.; Zhou, W. Study on the optimal charging strategy for lithium-ion batteries used in electric vehicles. *Energies* **2014**, *7*, 6783–6797. [[CrossRef](#)]
28. Liu, Y.-H.; Teng, J.-H.; Lin, Y.-C. Search for an optimal rapid charging pattern for lithium-ion batteries using ant colony system algorithm. *IEEE Trans. Ind. Electron.* **2005**, *52*, 1328–1336. [[CrossRef](#)]
29. Huang, J.-W.; Liu, Y.-H.; Wang, S.-C.; Yang, Z.-Z. Fuzzy-Control-Based Five-Step Li-Ion Battery Charger. In Proceedings of the International Conference on Power Electronics and Drive Systems (PEDS 2009), Taipei, Taiwan, 2–5 November 2009; IEEE: Piscataway, NJ, USA, 2009; pp. 1547–1551.
30. Lee, Y.-S.; Cheng, M.-W. Intelligent control battery equalization for series connected lithium-ion battery strings. *IEEE Trans. Ind. Electron.* **2005**, *52*, 1297–1307. [[CrossRef](#)]
31. Ho, Y.-H.; Huang, S.-S.; Liu, Y.-H.; Chiu, Y.-S.; Liu, C.-L. Optimization of a fuzzy-logic-control-based five-stage battery charger using a fuzzy-based taguchi method. *Energies* **2013**, *6*, 3528–3547.
32. Lyn, C.E.; Rahim, N.; Mekhilef, S. Dsp-Based Fuzzy Logic Controller for a Battery Charger. In Proceedings of the 2002 IEEE Region 10 Conference on Computers, Communications, Control and Power Engineering (TENCON'02), Beijing, China, 28–31 October 2002; IEEE: Piscataway, NJ, USA, 2002; pp. 1512–1515.
33. Hsieh, G.-C.; Chen, L.-R.; Huang, K.-S. Fuzzy-controlled li-ion battery charge system with active state-of-charge controller. *IEEE Trans. Ind. Electron.* **2001**, *48*, 585–593. [[CrossRef](#)]
34. Lee, Y.-S.; Cheng, M.-W.; Yang, S.-C. Fuzzy controlled individual cell equalizers for lithium-ion batteries. *IEICE Trans. Commun.* **2008**, *91*, 2380–2392. [[CrossRef](#)]
35. Mendel, J.M. Fuzzy logic systems for engineering: A tutorial. *Proc. IEEE* **1995**, *83*, 345–377. [[CrossRef](#)]
36. Kickert, W.J.; Mamdani, E.H. Analysis of a fuzzy logic controller. *Fuzzy Sets Syst.* **1978**, *1*, 29–44. [[CrossRef](#)]
37. Driankov, D.; Hellendoorn, H.; Reinfrank, M. Introduction. In *An Introduction to Fuzzy Control*; Springer: Berlin/Heidelberg, Germany, 1996; pp. 1–36.
38. Dunn, R.; Bell, K.; Daniels, A. Fuzzy logic and its application to power systems. In Proceedings of the IEE Colloquium on Artificial Intelligence Techniques in Power Systems (Digest No: 1997/354), London, UK, 3 November 1997; IET: Washington, DC, USA, 1997; pp. 4/1–4/4.
39. Samsung SDI Co., Ltd. *Specification of Product for Lithium-Ion Rechargeable Cell Model: Icr18650-26f*; Samsung SDI Co., Ltd.: Yongin-si, South Korea, 2009.
40. Díaz, J.; Martín-Ramos, J.A.; Pernía, A.M.; Nuño, F.; Linera, F.F. Intelligent and universal fast charger for ni-cd and ni-mh batteries in portable applications. *IEEE Trans. Ind. Electron.* **2004**, *51*, 857–863. [[CrossRef](#)]
41. Saberi, H.; Salmasi, F. Genetic optimization of charging current for lead-acid batteries in hybrid electric vehicles. In Proceedings of the International Conference on Electrical Machines and Systems (ICEMS), Seoul, South Korea, 8–11 October 2007; IEEE: Piscataway, NJ, USA, 2007; pp. 2028–2032.
42. Chen, L.-R.; Hsu, R.C.; Liu, C.-S. A design of a grey-predicted li-ion battery charge system. *IEEE Trans. Ind. Electron.* **2008**, *55*, 3692–3701. [[CrossRef](#)]

